Callaghan, S.; Filatov, M. A.; Savoie, H.; Boyle, R. W.; Senge, M. O. (2019):
In vitro cytotoxicity of a library of BODIPYanthracene and -pyrene dyads for application in photodynamic therapy.
Photochemical & Photobiological Sciences 18, 495–504. doi:10.1039/C8PP00402A

Journal Name

ARTICLE

In vitro Cytotoxicity of a Library of BODIPY-anthracene and -pyrene Dyads for Application in Photodynamic Therapy

Received 00th January 20xx,
Accepted 00th January 20xx

DOI: 10.1039/x0xx00000x

www.rsc.org/

Susan Callaghan,[a] Mikhail A. Filatov,[a] Huguette Savoie,[b] Ross W. Boyle,[b*] and M. O. Senge[c*]

The facile synthesis and *in vitro* activity of a library of heavy atom-free BODIPY-anthracene, -pyrene dyads (**BAD-13**–**BPyrD-19**) and a control (**BODIPY 20**) are reported. We demonstrate that singlet oxygen produced from dyad triplet states formed from charge-separated states is sufficient to induce cytotoxicity in human breast cancer cells (MDA-MB-468) at micromolar concentrations. The compounds in this series are promising candidates for photodynamic therapy, especially **BAD-17** which displays significant photocytotoxicity (15% cell viability) at a concentration of 5 × 10^{-7} M, with minimal toxicity (89% cell viability) in the absence of light.

Introduction

Photodynamic therapy (PDT) exploits the relationship between light of a specific wavelength, ground state triplet oxygen and a photoactive molecule to deliver a cytotoxic response mediated by singlet oxygen and other reactive oxygen species.[1] However, major drawbacks restrict the widespread application of PDT in clinical settings. These include, but are not limited to, photosensitivity post treatment, biocompatibility and large scale production of the photoactive molecule, and the development of photosensitizers with long-lived triplet states. Still, the phenomenon of photosensitization is universally studied and has been utilized in biomedical applications for centuries,[1a,2] and in recent decades BODIPY (boron-dipyrromethene)-based systems have established themselves as feasible agents for both phototherapy and diagnostics.[3] Moreover, the design of systems in which singlet oxygen generation can be modulated by different stimuli is also of increasing interest in the PDT community.[4]

Inherently, BODIPYs are chromophores, and therefore populate excited singlet states upon absorption of light.[5] Common design strategies employed to enhance intersystem crossing (ISC), and thus population of longer lived excited triplet states from which singlet oxygen is generated include halogenation,[6] dimerization[7] and conjugation to a spin converter e.g., C_{60}[8] (Fig. 1, compounds **1**, **2** and **4**). Additionally, aza-BODIPYs have been extensively studied for applications in PDT due to their red-shifted absorption spectra. Compound **3** is a highlight, both *in vitro* and *in vivo*, of the BODIPY-based PDT field with a reported 71% ablation of mammary tumors in a mouse model.[9]

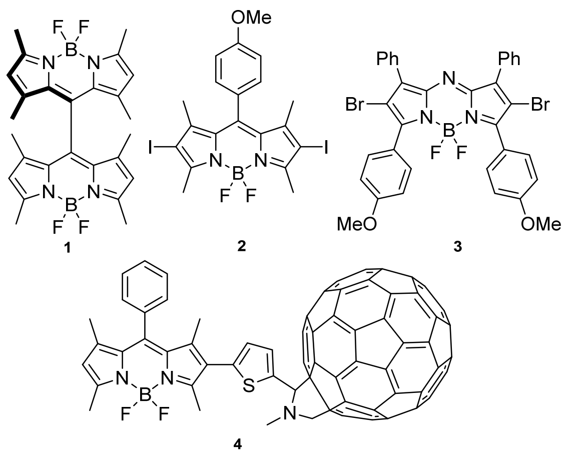

Figure 1 Examples of singlet oxygen-generating BODIPY-based compounds.

Our group has experience in the design and optimization of singlet oxygen sensitizers. Recently, we reported a family of BODIPY–anthracene, -pyrene and -perylene dyads (BAD, BPyrD) which produce triplet states *via* charge-separated states[10] generated by photo-induced electron transfer (PeT, Fig. 2 and Fig. 3).[11] We investigated the singlet oxygen quantum yields of these compounds, the most efficient being 67% in ethanol (Fig. 3, Table 1). Some of these exhibit a unique dual performance in triplet–triplet annihilation photon up-conversion (TTA-UC), either as a sensitizer or emitter component.[12]

We propose that these compounds have characteristics fundamental to PDT photosensitizers. Firstly, PeT is enhanced

[a] School of Chemistry, SFI Tetrapyrrole Laboratory, Trinity Biomedical Sciences Institute, Trinity College Dublin, The University of Dublin, 152-160 Pearse Street, Dublin 2, Ireland.
[b] Department of Chemistry, University of Hull, Cottingham Road, Kingston-upon-Hull HU6 7RX, United Kingdom, r.w.boyle@hull.ac.uk
[c] Medicinal Chemistry, Trinity Translational Medicine Institute, Trinity Centre for Health Sciences, Trinity College Dublin, The University of Dublin, St. James's Hospital, Dublin 8, Ireland. E-mail: sengem@tcd.ie

Electronic Supplementary Information (ESI) available: [details of experimental protocols, synthetic procedures and spectra]. See DOI: 10.1039/x0xx00000x in polar media due to stabilization of the charge-separated state, providing a singlet oxygen-generating mechanism (Table 1) that can be modulated.[10b,c] Moreover, as PeT is in competition with fluorescence, real time imaging of oxidative stress is possible.[10a]

These compounds are heavy atom-free, unlike other BODIPY chromophores suitable for PDT, and are expected to show high light/dark cytotoxicity ratios, similar to those observed in our previous test case.[10a] These compounds are also synthetically accessible and suitable for large scale production *via* acid-catalyzed condensation between the aryl aldehyde and either 2-methylpyrrole or 2,4-dimethylpyrrole, oxidation using DDQ

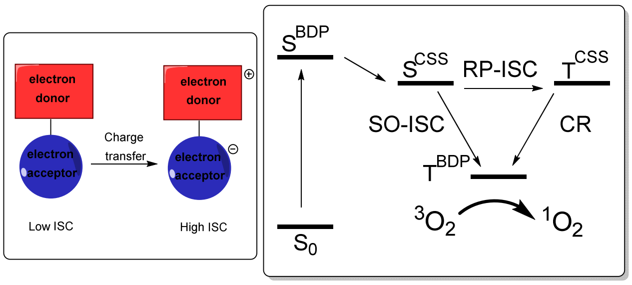

Figure 2 Schematic and Jablonski representation of ISC enhancement mediated by charge transfer. Electron acceptor: BODIPY core, electron donor: 8-substitution.

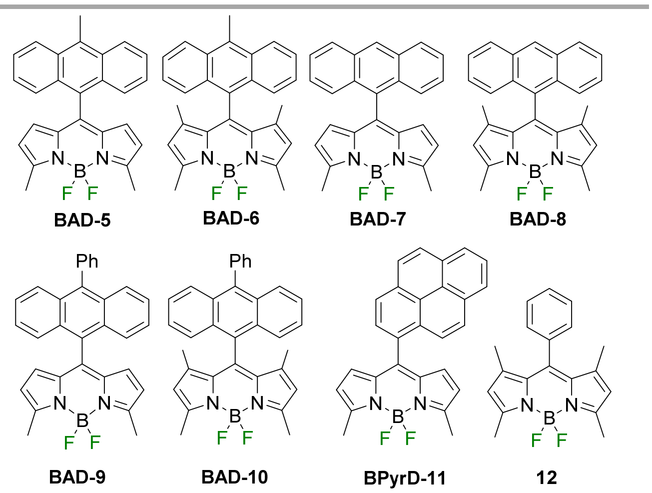

Figure 3 Structures of previously studied dyads with highest singlet oxygen quantum yields. Green indicates the site of modification in the current work.

Table 1: Singlet oxygen quantum yields of parent dyads in ethanol and hexane.‡ This work was carried out as part of previous studies.[10]

Compound	Φ_Δ EtOH	Φ_Δ Hexane
BAD-5	0.38	0.17
BAD-6	0.67	0.04
BAD-7	0.47	0.07
BAD-8	0.53	0.01
BAD-9	0.46	0.18
BAD-10	0.59	0.04
BPyrD-11	0.25	0.01
12	<0. 1	<0. 1

and boron insertion to yield the BODIPY in a one pot reaction.[10a] However, the parent BODIPYs are themselves insoluble in biological media and thus modification is required to realize their potential as PDT agents.

Results and discussion

In this body of work we translate our previous studies by providing a library of eight water-soluble compounds **BAD-13**–**BPyrD-19** and a control (**BODIPY 20**). To ascertain their applicability to PDT we have included *in vitro* evidence of cytotoxicity. The activity under biological conditions is presented and compared with singlet oxygen quantum yields of the parent and water-soluble BODIPYs in ethanol.

Firstly, we selected the parent BODIPYs with promising singlet oxygen quantum yields in polar solvents (Table 1) and synthesized them as previously described. We then introduced water-solubility using a two-step approach. Fluorine substitution with *N,N*-dimethylaminopropyne-1 units was followed by quaternization of the dimethylamino group with 1,3-propanesultone, which precipitated from the non-polar solvent, to afford compounds **BAD-13**–**BPyrD-19**, containing zwitterionic fragments that introduced water solubility (Fig. 4, Scheme 1).[13] For the cell biological studies, a control, **20**, bearing a phenyl group that cannot undergo the PeT process to produce singlet oxygen due to incompatible molecular orbital energies, was included (Fig. 4, Scheme 1). The series of water-soluble dyads were synthesized with substitution yields between 50–74% and quaternization yields between 45–94% (Fig. 4).

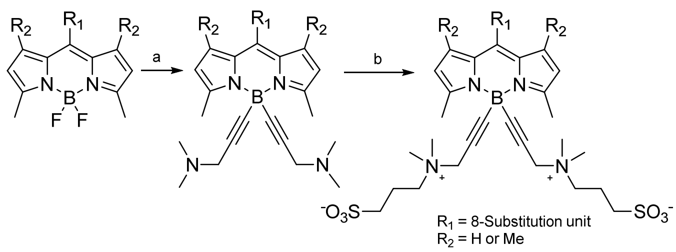

Scheme 1 General synthesis of water-soluble dyads. (a) 1. 3-Dimethylamino-1-propyne (4.5 eq.), n-BuLi (4 eq.), THF, rt, 30 min. 2. BAD, THF, rt, 2 h; (b) 1,3-propanesultone (6 eq.), EtOAc, 80 °C, 2 h. All parent and water-soluble BODIPYs synthesized are described in Fig. 3 and Fig 4., respectively.

Normalized absorption spectra for compounds **BAD-13**–compound **20** in water and ethanol are shown in Fig. 5. The two distinct units are evident with the anthracene or pyrene absorption maxima between 326 and 400 nm and the BODIPY unit absorbing between 501 and 527 nm (Table 2). The absorbance of anthracene is red-shifted compared to that of pyrene due to it having a smaller HOMO-LUMO gap.[10b] The compounds do not display significant changes in absorption maxima between the solvents, however a larger full width at half maxima is seen in water compared to ethanol due to the relative solvent polarity (Fig. 5).

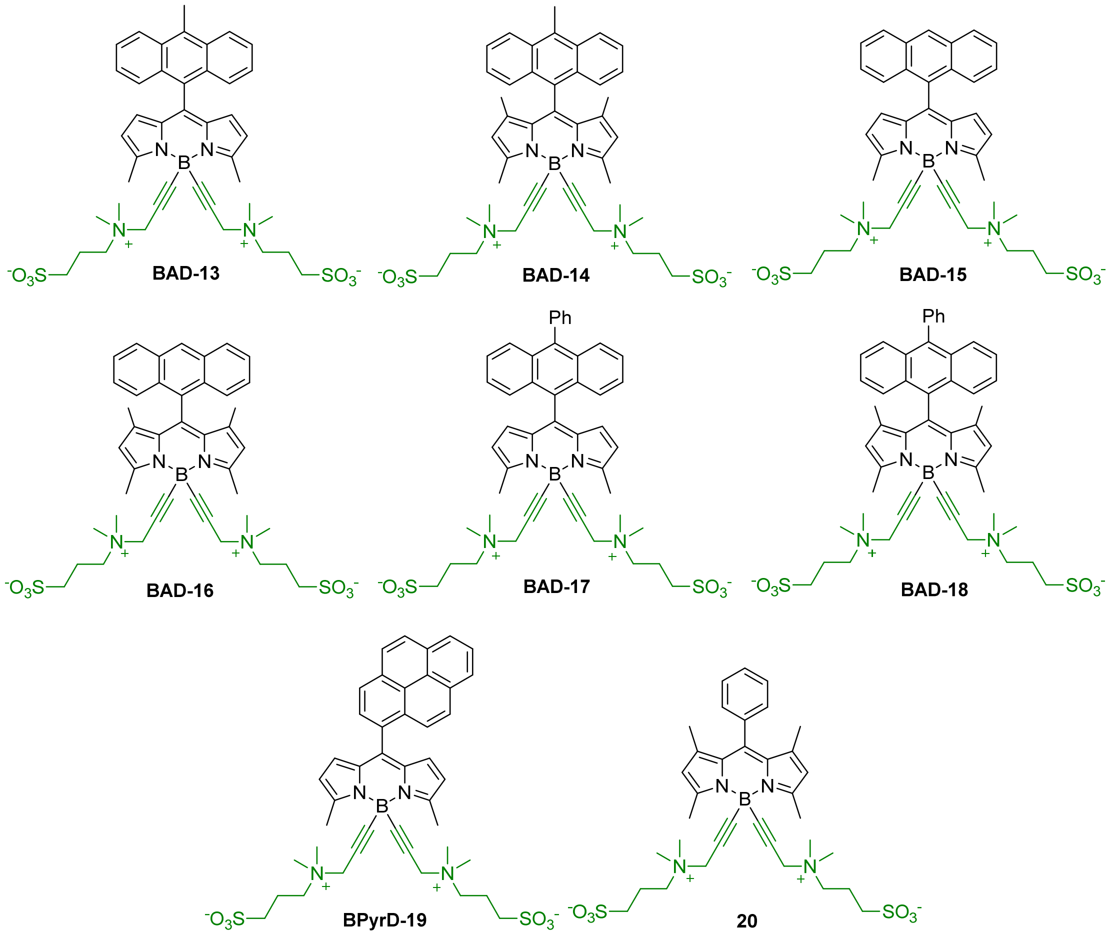

Figure 4 Library of water-soluble anthracene-, pyrene- or phenyl-BODIPY dyads. **BAD-13–BPyrD-19** are active compounds and **20** acts as a control. Green indicates the site of modification.

Table 2: Absorbance and emission maxima in water and ethanol and fluorescence quantum yields for **BAD-13–20** in water and ethanol.§

Compound	Absorption λ_{max} (H_2O)	Absorption λ_{max} (EtOH)	Emission λ_{max} (H_2O)	Emission λ_{max} (EtOH)	Φ_f (H_2O)	Φ_f (EtOH)
BAD-13	359, 376, 397, 512 nm	356, 375, 396, 514 nm	532 nm	530 nm	>0.01	>0.01
BAD-14	360, 378, 399, 502 nm	362, 379, 400, 505 nm	512 nm	514 nm	>0.01	>0.01
BAD-15	350, 367, 386, 511 nm	349, 366, 386, 514 nm	525 nm	523 nm	>0.01	>0.01
BAD-16	351, 368, 388, 501 nm	350, 368, 387, 504 nm	505 nm	510 nm	0.02	0.03
BAD-17	360, 377, 398, 527 nm	355, 373, 394, 514 nm	522 nm	525 nm	>0.01	>0.01
BAD-18	360, 378, 398, 506 nm	357, 374, 395, 504 nm	505 nm	511 nm	>0.01	0.01
BPyrD-19	329, 342, 511 nm	326, 342, 512 nm	511 nm	524 nm	>0.01	0.04
20	496 nm	500 nm	505 nm	508 nm	0.22	0.19

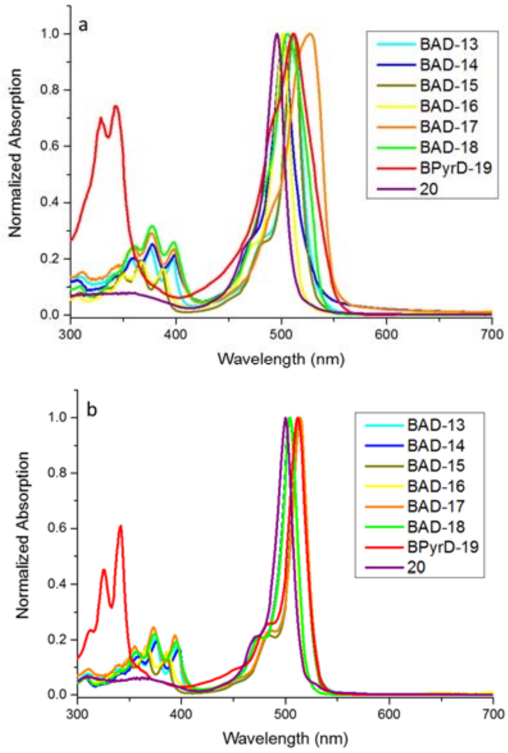

Figure 5 Normalized absorption spectra for compounds **BAD-13–20** in (a) water and (b) ethanol.

The fluorescence spectra and quantum yields are shown in Fig. 6 and Table 2. The quantum yields of the compounds were measured relative to the fluorescence of fluorescein in 0.1 M NaOH (ϕ_f = 0.95) and at a concentration of 1 × 10^{-5} M.[14] **BAD-13–BPyrD-19** display low fluorescence in both ethanol and water (<5%). This is expected as the PeT mechanism is in competition with fluorescence (Fig. 2). In contrast compound **20** displays relatively high fluorescence in both water and ethanol, 19% and 22% respectively, indicating that the triplet state is not as readily populated. We also observe lower fluorescence quantum yields in water compared to ethanol, due to the charge-separated state being stabilized to a greater extent in the more polar solvent. The same trend is not observed in **BAD–20**, which does not generate a charge-separated state (Fig. 6 and Table 2).

We then undertook singlet oxygen quantum yield studies of the water-soluble derivatives, **BAD-13–BPyrD-19** and a control (**BODIPY 20**) in water (Table 3), using a protocol adopted from literature (see SI).[15] Overall, they show comparable singlet oxygen quantum yields to that of the parent BODIPYs (**BAD-5–12**). Notably, control **20** displays negligible singlet oxygen generating abilities, as expected.

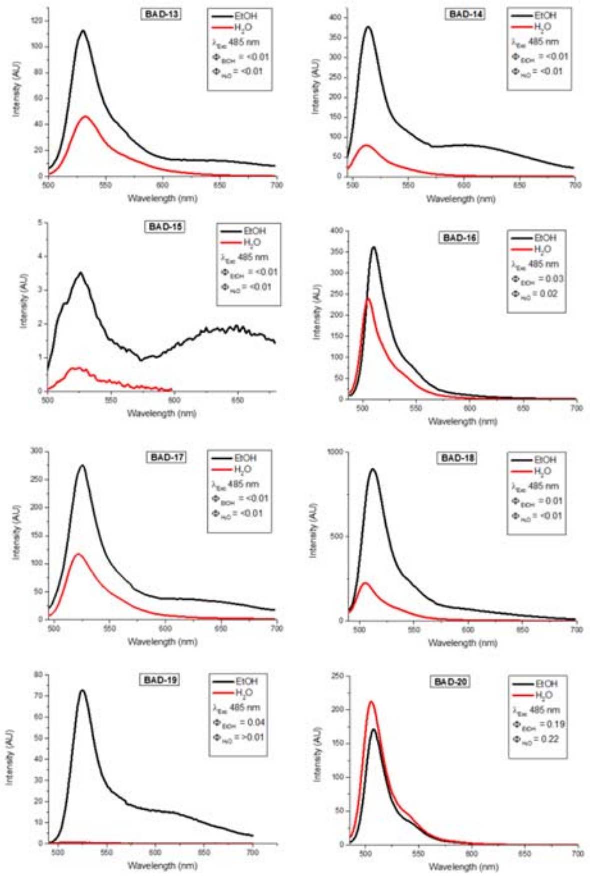

Figure 6 Emission spectra for compounds **BAD-13–20** in water (red) and ethanol (black). The quantum yields of the compounds were measured relative to the fluorescence of fluorescein in 0.1 M NaOH (ϕf = 0.95) and at a concentration of 1 × 10^{-5} M.[14]

Table 3: Singlet oxygen quantum yields of water-soluble dyads in ethanol and for comparison the singlet oxygen quantum yields of the parent dyads.‡ The singlet quantum yields of the parents were carried out as part of previous studies.[10]

Compound	Φ_Δ EtOH	Compound	Φ_Δ EtOH
BAD-5	0.38	**BAD-13**	0.38
BAD-6	0.67	**BAD-14**	0.52
BAD-7	0.47	**BAD-15**	0.64
BAD-8	0.53	**BAD-16**	0.39
BAD-9	0.46	**BAD-17**	0.48
BAD-10	0.59	**BAD-18**	0.66
BPyrD-11	0.25	**BPyrD-19**	0.03
12	<0. 1	**20**	0.02

To determine if photocytotoxicity could be observed, human breast cancer (MDA-MB-468) cells were incubated with compounds **BAD-13–20** at various concentrations (8 × 10^{-4} – 5 × 10^{-8} M) for 1 h. Following this, they were irradiated with broad-band visible light (400–700 nm, 23.8 mW cm^{-2}). The cells were then returned to the incubator for 24 h and an MTT assay was performed to determine cell viability (Fig. 7).[16] LC50 values were then calculated (Table 4).

Journal Name

ARTICLE

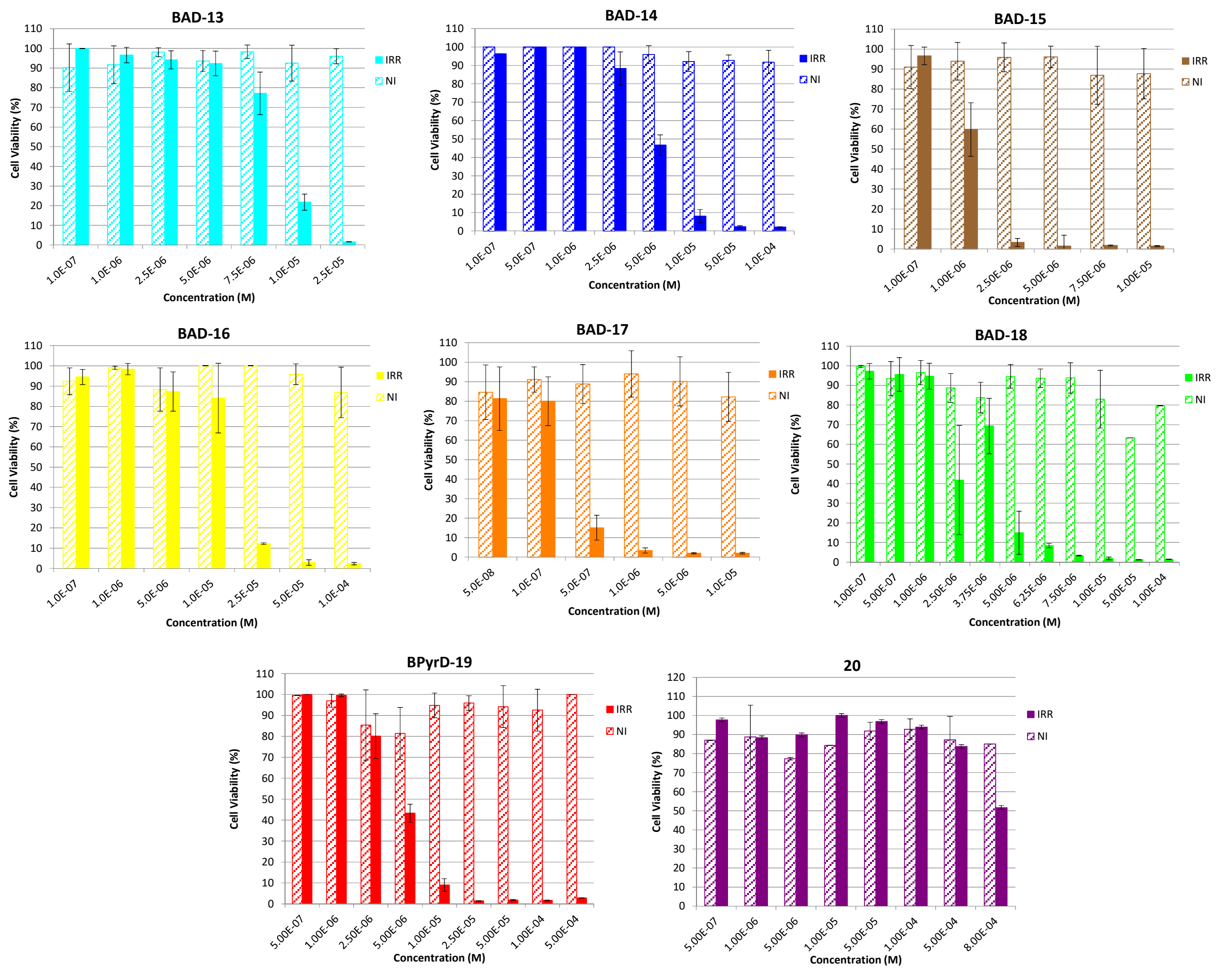

Figure 7 MDA-MB-468 cell viabilities after 1 h of incubation with **BAD-13–20** with and without light irradiation (400–700 nm, 20 J cm^{-2}) at various concentrations (8 × 10^{-4} –5 × 10^{-8} M).

Table 4: LD_{50} values for **BAD-13–20**.

Compound	LD_{50} Values (M)
BAD-13	8.7×10^{-6}
BAD-14	6.1×10^{-6}
BAD-15	1.3×10^{-6}
BAD-16	1.7×10^{-5}
BAD-17	2.8×10^{-7}
BAD-18	4.2×10^{-6}
BPyrD-19	5.26×10^{-6}
20	8.2×10^{-4}

BAD-13 and **BAD-14** have previously been investigated[10a] and are included as standards in this study. **BAD-6** has higher singlet oxygen quantum yield in ethanol (67%) when compared with **BAD-5** (38%). Similarly, **BAD-14** has a higher singlet oxygen quantum yield in ethanol (52%) when compared to **BAD-13** (38%) and this pattern is reflected in the *in vitro* studies. Although both **BAD-13** and **BAD-14** induced some degree of photocytotoxicity at micromolar concentrations, at the same concentration of 5 × 10^{-6} M the cell viability was reduced from 96% under dark conditions to 47% following illumination for **BAD-14** but there was a negligible reduction for **BAD-13** (Fig. 7). The LD_{50} values for **BAD-13** and **BAD-14** are 8.7 × 10^{-6} M and 6.1 × 10^{-6} M, respectively (Table 4).

BAD-15 and **BAD-16** contain anthracene at the 8 position of the BODIPY, resulting in a decrease in the HOMO (highest occupied molecular orbital) energy of the donor and thus has a slower rate of PeT compared to **BAD-13** and **BAD-14**.[10b] The

Please do not adjust margins

parent BODIPYs (**BAD-7** and **BAD-8**) are reported to have similar singlet oxygen quantum yields in ethanol, 47% and 53%, respectively. **BAD-15** has a singlet oxygen quantum yield in ethanol of 64% and **BAD-16** of 39 % (Table 3). **BAD-15** performed best and showed reduction in cell viability to 3% at 2.5×10^{-6} M (Fig. 7) and when directly compared to **BAD-14** at a concentration of 1×10^{-6} M shows improved photocytotoxicity (60% viability *vs* no reduction in cell viability). Additionally, **BAD-15** has lower LD_{50} value (1.3×10^{-6} M) than **BAD-13** and **BAD-14** (Table 4).

As we previously shown, **BAD-13** is able to undergo a cycloaddition reaction with self-sensitized singlet oxygen on the 9-methylanthracene subunit,[10a] which, may in part account for the reduced singlet oxygen quantum yield and lower cytotoxicity observed for this dyad. On the other hand, **BAD-15** and **BAD-16** are based on the unsubstituted anthracene which is known to possess rather low reactivity towards singlet oxygen, providing higher photostability and sensitization efficiency for these dyads.[17]

The phenylanthracene-based BODIPYs, **BAD-17** and **BAD-18,** again show micromolar and submicromolar activities under biological conditions and the parent BODIPYs (**BAD-9** and **BAD-10**) have similar singlet oxygen quantum yields of 46% and 59% in ethanol. **BAD-17** and **BAD-18** have singlet oxygen quantum yields in ethanol of 48% and 66%, respectively (Table 3). **BAD-17** has been identified as the best performing dyad of the study (LD_{50} value of 2.8×10^{-7} M, Table 4) with phototoxicity (89% cell viability under dark conditions *vs* 15% cell viability following irradiation) at 5×10^{-7} M (Fig. 7). In contrast, Fig. 7 shows that **BAD-14** does not display any photocytotoxicity at this concentration. Moreover, at a concentration of 5×10^{-6} M **BAD-18** effects a more profound reduction in cell viability (15%) when compared to the standard **BAD-14** (47% viability).

In addition to the anthracene derivatives, we also tested a pyrene-BODIPY dyad, **BPyrD-19**, which also showed cell phototoxicity and a singlet oxygen quantum yield in ethanol of only 3%. The parent BODIPY was previously shown to have a singlet oxygen quantum yield of 25% in ethanol. At a concentration of 1×10^{-5} M there is a reduction in cell viability from 95% to 9% post illumination. At a lower concentration of 5×10^{-6} M significant photocytotoxicity (43% viability) is also observed (Fig. 7). The efficiency of this photosensitizer is similar to that of **BAD-14,** which at a dyad concentration of 5×10^{-6} M has a reduction in cell viability to 46% following light activation (Fig. 7).

The final compound tested was the control, **20**, which did not display significant sensitization in ethanol. As seen in Fig. 7, there is nominal photocytotoxicity at appreciable concentrations with an LD_{50} value of 8.2×10^{-4} M. However, there was a moderate decrease in cell viability (85% *vs* 52%) at the highest concentration of 8×10^{-4} M when light was introduced. This would indicate that photosensitization does take place at high concentration but overall, there is minimal phototoxicity and thus PDT is in fact the predominant mechanism for cell toxicity observed in the active compounds. Importantly, this experiment also shows that the water-soluble aryl-BODIPYs are not inherently toxic at the concentrations under investigation.

Conclusions

A series of synthetically accessible heavy atom-free water-soluble aryl-BODIPY photosensitizers were synthesized using condensation, fluorine substitution and quaternization reactions. Extensive *in vitro* analysis was performed and we have shown varying photocytotoxicity efficiencies resulting from singlet oxygen produced *via* a PeT mechanism. The cytotoxicity studies show that all active compounds cause a reduction in cell viability after illumination and minimal dark toxicity (Fig. 7 and Table 4). These light-to-dark ratios are an important property for the development of successful photosensitizers as they contribute to tackling generalized photosensitivity which plagues current PDT regimes.[18]

Although the singlet oxygen quantum yields of the water-soluble BODIPYs in ethanol cannot fully account for the *in vitro* activities as factors including cell uptake have not been considered in the present study, we see similar patterns of toxicity that are consistent with the synthetic tunability of this family of compounds. This is further validated by the negligible activity of the control compound, **20**, *in vitro*. The control experiment as well as the light-to-dark ratios has also consolidated that the water-soluble aryl-BODIPYs do not have inherent toxicity and that singlet oxygen generation is the predominant mechanism of action.

We have shown that three BADs (**BAD-15**, **BAD-17**, **BAD-18**) have higher toxicity in comparison to the standard, **BAD-14** (LD_{50} value = 6.1×10^{-6} M). In particular, the submicromolar activity of **BAD-17** (LD_{50} value = 2.8×10^{-7} M) is significantly more potent than **BAD-14**. This enhancement has considerable consequences for photosensitizer dosage. Coupled with the compounds low light-to-dark toxicity ratios, long-lived triplet state and synthetic accessibility makes it a target for future exploration. We intend to continue the development of this class of photosensitizer with cell uptake and localization studies, *in vivo* studies and by optimizing our compounds to feature more red-shifted absorption spectra.

Experimental

Materials and Methods

Unless otherwise specified, all chemicals including 10-methylanthracene-9-carboxaldehyde, anthracene-9-carbaldehyde, benzaldehyde, pyrene-1-carboxaldehyde and 2,4-dimethylpyrrole were sourced commercially and used without further purification. The synthetic procedures were adapted from literature and characterized accordingly as follows: 3,5-dimethyl-8-(10-methylanthracen-9-yl)-4,4-difluoro-4-bora-3a,4a-diaza-*s*-indacene, **BAD-5**,[10a] 1,3,5,7-tetramethyl-8-(10-methylanthracen-9-yl)-4,4-difluoro-4-bora-3a,4a-diaza-*s*-indacene, **BAD-6**,[19] 3,5-dimethyl-8-(10-methylanthracen-9-yl)-4,4-(3-(dimethylamino)prop-1-yn-1-yl)-4-bora-3a,4a-diaza-*s*-indacene, **BAD-21**, 1,3,5,7-tetramethyl-8-(10-methylanthracen-9-yl)-4,4-(3-(dimethylamino)prop-1-yn-1-yl)-4-bora-3a,4a-diaza-*s*-indacene, **BAD-22**, 3,3'-(((3,5-dimethyl-8-(10-methylanthracen-9-yl)-4-bora-3a,4a-diaza-*s*-indacene-4,4-diyl)bis(prop-2-yne-3,1-diyl))bis(dimethylammoniumdiyl))bis(propane-1-sulfonate), **BAD-13**, 3,3'-(((1,3,5,7-tetramethyl-8-(10-methylanthracen-9-yl)-4-bora-3a,4a-diaza-*s*-indacene-4,4-diyl)bis(prop-2-yne-3,1-diyl))bis(dimethylammoniumdiyl))bis(propane-1-sulfonate), **BAD-14**,[10a] 2-methylpyrrole,[20] 10-phenylanthracene-9-carbaldehyde,[10c, 21] 3,5-dimethyl-8-(anthracen-9-yl)-4,4-difluoro-4-bora-3a,4a-diaza-*s*-indacene, **BAD-7**,[10b] 1,3,5,7-tetramethyl-8-

(anthracen-9-yl)-4,4-difluoro-4-bora-3a,4a-diaza-*s*-indacene, **BAD-8**,[19] 3,5-dimethyl-8-(10-phenylanthracen-9-yl)-4,4-difluoro-4-bora-3a,4a-diaza-*s*-indacene, **BAD-9**, 1,3,5,7-tetramethyl-8-(10-phenylanthracen-9-yl)-4,4-difluoro-4-bora-3a,4adiaza-*s*-indacene, **BAD-10**,[10b] 3,5-dimethyl-8-(pyrene-1-yl)-4,4-difluoro-4-bora-3a,4a-diaza-*s*-indacene, **BPhyD-11**,[10c] 1,3,5,7-tetramethyl-8-(phenyl-9-yl)-4,4-difluoro-4-bora-3a,4a-diaza-*s*-indacene, **12**.[22]

All air and/or water sensitive materials were handled using standard high vacuum techniques. Dry THF and DCM were obtained by passing through alumina under N_2 in a solvent purification system and then further dried over activated molecular sieves. Analytical thin-layer chromatography was performed using silica gel 60 (fluorescence indicator F254, pre-coated sheets, 0.2 mm thick, 20 cm × 20 cm; Merck) plates and visualized by UV irradiation (λ = 254 nm). Column chromatography was carried out using Fluka Silica Gel 60 (230–400 mesh; Merck). UV/Vis spectra were recorded in solutions using a Specord 250 spectrophotometer from Analytic Jena (1 cm path length quartz cell). Fluorescence spectra were measured on a Cary Eclipse Fluorescence Spectrometer. NMR spectra were recorded on a Bruker AV 600, Bruker Advance III 400 MH or a Bruker DPX400 400 MHz or an Agilent 400 spectrometer. Accurate mass measurements (HRMS) were carried out using a Bruker microTOF-Q™ ESI-TOF mass spectrometer. Mass spectrometry was performed with a Q-Tof Premier Waters MALDI quadrupole time-of-flight (Q-TOF) mass spectrometer equipped with Z-spray electrospray ionization (ESI) and matrix assisted laser desorption ionization (MALDI) sources in positive mode with trans-2-[3-(4-tert-butylphenyl)-2-methyl-2-propenylidene]malononitrile as the matrix. Melting points were measured using an automated melting point machine, SMP50 (Stuart).

Synthetic procedures

General Procedure A: Fluorine substitution.

To a solution of 3-dimethylamino-1-propyne (4.5 eq.) in dry THF was added *n*-BuLi (4 eq.). The mixture was stirred at rt for 30 min. BODIPY (1 eq.) dissolved in dry THF was added drop-wise to the reaction and the reaction was stirred at rt for 2 h. The reaction was quenched with H_2O and concentrated. The residue was dissolved in DCM, washed with H_2O (3 × 100 mL) and extracted with DCM (3 × 100 mL). The product was purified by silica gel column chromatography (DCM/MeOH, 10:1).

General Procedure B: Sulfobetaine formation.

Dimethylaminopropyne-substituted dyad (1 eq.) was dissolved in EtOAc and the solution was heated to reflux under argon. A solution of 1,3-propanesultone (6 eq.) in EtOAc (2 mL) was added and the reaction mixture was refluxed for 2 h. After cooling to rt the precipitate formed was filtered and carefully washed with Et_2O. The obtained product was dried at 80 °C.

Experimental Detail

3,5-Dimethyl-8-(anthracen-9-yl)-4,4-(3-(dimethylamino)prop-1-yn-1-yl)-4-bora-3a,4a-diaza-*s*-indacene, BAD-23: BAD-23 was synthesized in accordance with general procedure A using 3-dimethylamino-1-propyne (377 mg, 4.55 mmol), dry THF (20 mL), *n*-BuLi (258 mg, 4.04 mmol) and **BAD-7** (400 mg, 1.01 mmol) dissolved in dry THF (50 mL) to yield an orange solid (388 mg, 7.43 × 10^{-4} mol, 74%). M.p. >250 °C; R_f = 0.69 (DCM/MeOH, 9:1); ^{1}H NMR (400 MHz, $CDCl_3$): δ = 8.55 (s, 1H, CH_{Ar}), 8.01 (d, *J* = 8.5 Hz, 2H, CH_{Ar}), 7.84 (dd, *J* = 8.7, 0.8 Hz, 2H, CH_{Ar}), 7.47 – 7.41 (m, 2H, CH_{Ar}), 7.35 (m, 2H, CH_{Ar}), 6.19 – 6.07 (m, 4H, $CH_{pyrrole}$), 3.31 (s, 4H, CH_2), 2.89 (s, 6H CH_3), 2.35 ppm (s, 12H, NCH_3); ^{13}C NMR (101 MHz, $CDCl_3$): δ = 157.3, 139.4, 134.3, 130.9, 130.8, 128.2, 128.1, 128.0, 127.9, 126.4, 126.3, 125.4, 119.8, 49.1, 44.2, 16.4 ppm; UV/Vis (DCM): λ_{max} (log ε) = 349 (4.22), 366 (4.34), 386 (4.28), 513 nm (5.11); HRMS (ESI) *m/z* calcd. for $C_{35}H_{36}BN_4$ $[M+H]^+$: 523.2574, 523.2594 found.

3,5-(((Dimethyl-8-(anthracen-9-yl)-4-bora-3a,4a-diaza-*s*-indacene-4,4-diyl)bis(prop-2-yne-3,1-diyl))bis(dimethylammoniumdiyl))bis(propane-1-sulfonate), BAD-15: BAD-15 was synthesized in accordance with general procedure B using **BAD-23** (250 mg, 4.79 × 10^{-4} mol), EtOAc (100 mL) and 1,3-propanesultone (350 mg, 2.81 mmol) to yield an orange solid (261 mg, 3.40 × 10^{-4} mol, 71%). M.p. >250 °C; ^{1}H NMR (400 MHz, DMSO-d_6): δ = 8.79 (s, 1H, CH_{Ar}), 8.17 (d, *J* = 8.3 Hz, 2H, CH_{Ar}), 7.66 (d, *J* = 8.3 Hz, 2H, CH_{Ar}), 7.54.72 – 7.46 (m, 4H, CH_{Ar}), 6.35 (dd, *J* = 11.7, 4.2 Hz, 2H, $CH_{pyrrole}$), 6.16 (dd, J = 11.7, 4.2 Hz, 2H, $CH_{pyrrole}$), 4.44 (m, 4H, CH_2), 3.65 – 3.58 (m, 4H, CH_2), 3.18 – 3.17 (m, 12H, NCH_3), 2.85 (s, 6H, CH_3), 2.62 – 2.59 (m, 4H, CH_2), 2.17 – 2.13 ppm (m, 4H CH_2); ^{13}C NMR (101 MHz, DMSO-d_6): δ = 158.1, 157.8, 134.3, 130.9, 130.7, 128.9, 128.7, 125.9, 125.7, 121.0, 63.3, 50.2, 50.0, 48.3, 43.9, 19.6, 16.7, 16.5 ppm; UV/Vis (MeOH): λ_{max} (log ε) = 347 (4.70), 365 (4.83), 384 (4.76), 511 nm (5.56); HRMS (ESI) *m/z* calcd. for $C_{41}H_{47}BN_4NaO_6S_2$ $[M+Na]^+$: 789.2929, 789.2932 found.

1,3,5,7-Tetramethyl-8-(anthracen-9-yl)-4,4-(3-(dimethylamino)prop-1-yn-1-yl)-4-bora-3a,4a-diaza-*s*-indacene, BAD-24: BAD-24 was synthesized in accordance with general procedure A using 3-dimethylamino-1-propyne (352 mg, 4.25 mmol), dry THF (20 mL), *n*-BuLi (241 mg, 3.77 mmol) and **BAD-8** (400 mg, 9.43 × 10^{-4} mol) dissolved in dry THF (50 mL) to yield an orange solid (303 mg, 5.51 × 10^{-4} mol, 59%). M.p. >250 °C; R_f = 0.50 (DCM/MeOH, 9:1); ^{1}H NMR (400 MHz, $CDCl_3$): δ = 8.55 (s, 1H, CH_{Ar}), 8.01 (d, *J* = 8.3 Hz, 2H, CH_{Ar}), 7.90 (d, *J* = 8.7 Hz, 2H, CH_{Ar}), 7.52 – 7.43 (m, 2H, CH_{Ar}), 7.42 – 7.35 (m, 2H, CH_{Ar}), 5.92 (s, 2H, $CH_{pyrrole}$), 3.44 – 3.22 (m, 4H, CH_2), 2.82 (s, 6H, $CH_{3pyrrole}$), 2.38 – 2.36 (m, 12H, NCH_3), 0.61 ppm (s, 6H, $CH_{3pyrrole}$); ^{13}C NMR (101 MHz, $CDCl_3$): δ = 155.3, 140.6, 138.7, 131.3, 130.4, 129.8, 129.0, 128.2, 128.0, 126.8, 125.7, 125.3, 121.4, 49.0, 44.1, 16.3, 13.5 ppm; UV/Vis (DCM): λ_{max} (log ε) = 504 (5.20), 388 (4.33), 368 (4.40), 350 nm (4.25); HRMS (ESI): *m/z* calcd. for $C_{37}H_{40}BN_4$ $[M+H]^+$: 551.3347, 551.3343 found.

3,3'-(((1,3,5,7-Tetramethyl-8-(anthracen-9-yl)-4-bora-3a,4a-diaza-*s*-indacene-4,4-diyl)bis(prop-2-yne-3,1-diyl))bis(dimethylammoniumdiyl))bis(propane-1-sulfonate), BAD-16*:* BAD-16 was synthesized in accordance with general procedure B using **BAD-24** (200 mg, 3.62 × 10^{-4} mol), EtOAc (100 mL) and 1,3-propanesultone (265 mg, 2.17 mmol) to yield an orange solid (277 mg, 3.49 × 10^{-4} mol, 95%). M.p. >250 °C; ^{1}H NMR (400 MHz, DMSO-d_6): δ = 8.85 (s, 1H, CH_{Ar}), 8.20 – 8.18 (m, 2H, CH_{Ar}), 7.68 – 7.61 (m, 2H, CH_{Ar}), 7.60 – 7.47 (m, 4H, CH_{Ar}), 6.17 (s, 2H, $CH_{pyrrole}$), 4.39 – 4.37 (m, 4H, CH_2), 3.58 – 3.45 (m, 4H, CH_2), 3.10 (s, 12H, NCH_3), 2.73 (s, 6H, CH_3), 2.53 – 2.49 (m, 4H, CH_2), 2.07 – 2.03 (m, 4H, CH_2), 0.55 ppm (s, 6H, $CH_{3pyrrole}$); ^{13}C NMR (101 MHz, DMSO-d_6): δ = 156.0, 141.1, 139.1, 131.3, 130.3, 129.3, 128.1, 126.4, 124.3, 122.6, 63.2, 55.1, 50.2, 48.4, 19.5, 16.5, 13.4 ppm; UV/Vis (MeOH): λ_{max} (log ε) = 502 (4.99), 386 (4.19), 366 (4.25), 349 nm (4.11); HRMS (ESI): *m/z* calcd. for $C_{43}H_{51}BN_4NaO_6S_2$ $[M+Na]^+$: 817.3243, 817.3259 found.

3,5-Dimethyl-8-(10-phenylanthracen-9-yl)-4,4-(3-(dimethylamino)prop-1-yn-1-yl)-4-bora-3a,4a-diaza-*s*-indacene, BAD-25: BAD-25 was synthesized in accordance with general procedure A using 3-dimethylamino-1-propyne (336 mg, 4.05 mmol), dry THF (20 mL), *n*-BuLi (230 mg, 3.60 mmol) and **BAD-9** (400 mg, 8.99 × 10^{-4} mol) dissolved in dry THF (50 mL) to yield an orange solid (330 mg, 5.51 × 10^{-4} mol, 61%). M.p. >250 °C; R_f = 0.54 (DCM/MeOH, 9:1); ^{1}H NMR (400 MHz, $CDCl_3$): δ = 7.93 – 7.85 (m, 2H, CH_{Ar}), 7.70 – 7.64 (m, 2H, CH_{Ar}), 7.63 – 7.53 (m, 3H, CH_{Ar}), 7.49 – 7.45 (m, 2H, CH_{Ar}), 7.37 – 7.27 (m, 4H, CH_{Ar}), 6.23 (d, *J* = 4.2 Hz, 2H, $CH_{pyrrole}$), 6.17 (d, *J* = 4.2 Hz, 2H, $CH_{pyrrole}$), 3.36 (s, 4H, CH_2), 2.90 (s, 6H, $CH_{3pyrrole}$), 2.39 ppm (s, 12H, NCH_3); ^{13}C NMR (101 MHz, $CDCl_3$): δ = 157.3, 139.8, 138.9, 138.5, 134.5, 131.1, 130.5, 129.4, 128.4, 128.1, 127.9, 127.7, 126.9, 126.6, 126.0, 125.2, 119.9, 49.0, 44.1, 16.4 ppm; UV/Vis (DCM): λ_{max} (log ε) = 355 (4.35), 374 (4.50), 395 (4.43), 512 nm (4.85); HRMS (ESI) *m/z* calcd. for $C_{41}H_{40}BN_4$ $[M+H]^+$: 599.3348, 599.3347 found.

3,5-(((Dimethyl-8-(10-phenylanthracen-9-yl)-4-bora-3a,4a-diaza-*s*-indacene-4,4-diyl)bis(prop-2-yne-3,1-diyl))bis(dimethylammoniumdiyl))bis(propane-1-sulfonate), BAD-17: BAD-17 was synthesized in accordance with general procedure B using **BAD-25** (250 mg, 4.18 × 10^{-4} mol), EtOAc (100 mL) and 1,3-propanesultone (306 mg, 2.59 mmol) to yield an orange solid (191 mg, 2.30 × 10^{-4} mol, 55%). M.p. >250 °C; ^{1}H NMR (400 MHz, DMSO-d$_6$): δ = 7.70 – 7.62 (m, 4H, CH_{Ar}), 7.62 – 7.55 (m, 3H, CH_{Ar}), 7.51 – 7.44 (m, 4H, CH_{Ar}), 7.43 – 7.38 (m, 2H, CH_{Ar}), 6.39 (dd, *J* = 11.1, 4.3 Hz, 2H, $CH_{pyrrole}$), 6.24 (dd, *J* = 11.0, 4.2 Hz, 2H, $CH_{pyrrole}$), 4.41 – 4.37 (m, 4H, CH_2), 3.58 – 3.48 (m, 4H, CH_2), 3.10 (s, 12H, NCH_3), 2.82 – 2.81 (m, 6H, $CH_{3pyrrole}$), 2.51 – 2.49 (m, 4H, CH_2), 2.09 – 2.04 ppm (m, 4H, CH_2); ^{13}C NMR (101 MHz, DMSO-d$_6$): δ = 134.3, 131.2, 130.3, 129.8, 129.1, 128.4, 127.1, 126.1, 127.0, 50.3, 50.1, 48.3, 40.5, 40.2, 40.0, 39.8, 39.4, 39.3, 19.5, 16.5, 16.7 ppm; UV/Vis (MeOH): λ_{max} (log ε) = 354 (4.29), 371 (4.44), 392 (4.38), 511 nm (5.08); HRMS (MALDI) *m/z* calcd. for $C_{47}H_{52}BN_4O_6S_2$ $[M+H]^+$: 843.3421, 843.3444 found.

1,3,5,7-Tetramethyl-8-(10-phenylanthracen-9-yl)-4,4-(3-(dimethylamino)prop-1-yn-1-yl)-4-bora-3a,4a-diaza-*s*-indacene, BAD-26: BAD-26 was synthesized in accordance with general procedure A using 3-dimethylamino-1-propyne (299 mg, 3.60 mmol), dry THF (20 mL), *n*-BuLi (205 mg, 3.20 mmol) and **BAD-10** (400 mg, 8.00 × 10^{-4} mol) dissolved in dry THF (50 mL) to yield an orange solid (250 mg, 3.99 × 10^{-4} mol, 50%). M.p. >250 °C; R_f = 0.42 (DCM/MeOH, 9:1); ^{1}H NMR (400 MHz, $CDCl_3$): δ = 7.95 (d, J = 8.4 Hz, 2H, CH_{Ar}), 7.66 (d, *J* = 8.4 Hz, 2H, CH_{Ar}), 7.61 – 7.53 (m, 3H, CH_{Ar}), 7.46 – 7.44 (m, 2H, CH_{Ar}), 7.40 – 7.29 (m, 4H, CH_{Ar}), 5.95 (s, 2H, $CH_{pyrrole}$), 3.35 (s, 4H, CH_2), 2.84 (s, 6H, $CH_{3pyrrole}$), 2.39 (s, 12H, NCH_3), 0.72 ppm (s, 6H, $CH_{3pyrrole}$); ^{13}C NMR (101 MHz, $CDCl_3$): δ = 155.3, 140.7, 139.2, 139.1, 138.4, 131.3, 130.6, 129.9, 129.4, 128.9, 128.4, 127.7, 126.9, 126.5, 125.5, 125.4, 121.5, 89.2, 49.0, 44.0, 29.7, 16.3, 13.6 ppm; UV/Vis (DCM): λ_{max} (log ε) = 356 (4.31), 375 (4.46), 396 (4.40), 504 nm (5.15); HRMS (ESI) *m/z* calcd. for $C_{43}H_{44}BN_4$ $[M+H]^+$: 627.3661, 627.3671 found.

1,3,5,7-(((Tetramethyl-8-(10-phenylanthracen-9-yl)-4-bora-3a,4a-diaza-*s*-indacene-4,4-diyl)bis(prop-2-yne-3,1-diyl))bis(dimethylammoniumdiyl))bis(propane-1-sulfonate), BAD-18: BAD-18 was synthesized in accordance with general procedure B using **BAD-26** (200 mg, 3.19 × 10^{-4} mol), EtOAc (100 mL), 1,3-propanesultone (234 mg, 1.92 mmol) to yield an orange solid (148 mg, 1.71 × 10^{-4} mol, 54%). M.p. >250 °C; ^{1}H NMR (400 MHz, DMSO-d$_6$): δ = 7.72 – 7.69 (m, 2H, CH_{Ar}), 7.66 – 7.61 (m, 3H, CH_{Ar}), 7.50 – 7.57 (m, 2H, CH_{Ar}), 7.55 – 7.47 (m, 2H, CH_{Ar}), 7.47 – 7.41 (m, 4H, CH_{Ar}), 6.19 (s, 2H, $CH_{pyrrole}$), 4.39 – 4.37 (m, 4H, CH_2), 3.54 – 3.50 (m, 4H, CH_2), 3.09 (d, J = 18.1 Hz, 12H, NCH_3), 2.74 (s, 6H, $CH_{3pyrrole}$), 2.50 – 2.47 (m, 4H, CH_2), 2.07 – 2.03 (m, 4H, CH_2), 0.64 ppm (s, 6H, $CH_{3pyrrole}$); ^{13}C NMR (101 MHz, DMSO-d$_6$): δ = 156.1, 141.2, 139.6, 139.2, 137.8, 131.4, 130.4, 129.7, 129.2, 129.1, 127.9, 127.8, 127.1, 126.6, 124.6, 122.7, 84.7, 63.2, 55.1, 50.2, 48.9, 48.4, 45.2, 42.2, 29.3, 19.5, 16.5, 13.4 ppm; UV/Vis (MeOH): λ_{max} (log ε) = 355 (4.07), 372 (4.22), 393 (4.17), 502 nm (4.85); HRMS (ESI) *m/z* calcd. for $C_{49}H_{55}BN_4NaO_6S_2$ $[M+Na]^+$: 893.3557, 893.3568 found.

3,5-Dimethyl-8-(pyrene-9-yl)-4,4-(3-(dimethylamino)prop-1-yn-1-yl)-4-bora-3a,4a-diaza-*s*-indacene, BPyrD-27: BPyrD-27 was synthesized in accordance with general procedure A using 3-dimethylamino-1-propyne (267 mg, 3.21 mmol), dry THF (20 mL), *n*-BuLi (183 mg, 2.86 mmol) and **BPyrD-11** (300 mg, 7.14 × 10^{-4} mol) dissolved in dry THF (50 mL) to yield an orange solid (232 mg, 4.23 × 10^{-4} mol, 60%). M.p. >250 °C; R_f = 0.58 (DCM/MeOH, 9:1); ^{1}H NMR (400 MHz, $CDCl_3$): δ = 8.27 – 7.92 (m, 9H, CH_{Ar}), 6.37 (d, *J* = 3.9 Hz, 2H, $CH_{pyrrole}$), 6.23 (d, *J* = 3.9 Hz, 2H, $CH_{pyrrole}$), 3.35 – 3.31 (m, 4H, CH_2), 2.91 (s, 6H, $CH_{3pyrrole}$), 2.40 – 2.37 ppm (m, 12H, NCH_3); ^{13}C NMR (101 MHz, $CDCl_3$): δ = 157.2, 140.9, 134.1, 131.8, 131.2, 130.8, 130.4, 129.0, 128.5, 128.3, 127.9, 127.2, 126.3, 125.7, 125.6, 125.5, 124.4, 124.3, 123.8, 119.7, 49.0, 44.1, 16.4 ppm; UV/Vis (DCM): λ_{max} (log ε) = 311 (4.38), 325 (4.66), 342 (4.77), 511 nm (5.02); HRMS (ESI) *m/z* calcd. for $C_{37}H_{36}BN_4$ $[M+H]^+$: 547.3034, 547.3034 found.

3,3'-(((3,5-Dimethyl-8-(pyrene-9-yl)-4-bora-3a,4a-diaza-*s*-indacene-4,4-diyl)bis(prop-2-yne-3,1-diyl))bis(dimethylammoniumdiyl))bis(propane-1-sulfonate), BPyrD-19: BPyrD-19 was synthesized in accordance with general procedure B using **BPyrD-27** (175 mg, 3.20 × 10^{-4} mol) and EtOAc (100 mL), 1,3-propanesultone (235 mg, 1.92 mmol) to yield an orange solid (225 mg, 2.85 × 10^{-4} mol, 89%). M.p. >250 °C; ^{1}H NMR (400 MHz, DMSO-d$_6$): δ = 8.39 (t, *J* = 8.4 Hz, 2H, CH_{Ar}), 8.32 – 8.24 (m, 3H, CH_{Ar}), 8.18 – 8.06 (m, 3H, CH_{Ar}), 7.82 – 7.77 (m, 1H, CH_{Ar}), 6.50 – 6.37 (m, 4H, $CH_{pyrrole}$), 4.45 – 4.31 (m, 4H, CH_2), 3.62 – 3.45 (m, 4H, CH_2), 3.10 – 3.07 (m, 12H, NCH_3), 2.80 (m, 6H, $CH_{3pyrrole}$), 2.69 – 2.59 (m, 4H, CH_2), 2.09 – 2.00 ppm (m, 4H, CH_2); ^{13}C NMR (101 MHz, DMSO-d$_6$) δ = 150.0, 133.9, 126.3, 124.6, 123.7, 123.0, 122.5, 121.7, 120.8, 120.4, 120.0, 119.3, 118.7, 118.2, 117.9, 116.6, 116.2, 112.6, 63.2, 55.2, 47.6, 42.2, 40.7, 20.6, 17.3, 11.1, 8.0 ppm; UV/Vis (MeOH): λ_{max} (log ε) = 311 (4.25), 323 (4.52), 339 (4.66), 509 nm (4.87); HRMS (ESI) *m/z* calcd. for $C_{43}H_{46}BN_4O_6S_2$ $[M-H]^-$: 789.2965, 789.2957 found.

1,3,5,7-Tetramethyl-8-(phenyl-9-yl)-4,4-(3-(dimethylamino)prop-1-yn-1-yl)-4-bora-3a,4a-diaza-*s*-indacene, 28: Compound **28** was synthesized in accordance with general procedure A using 3-dimethylamino-1-propyne (230 mg, 2.78 mmol), dry THF (20 mL), *n*-BuLi (158 mg, 2.46 mmol) and 12 (200 mg, 6.17×10^{-4} mol) dissolved in dry THF (50 mL) to yield an orange solid (191 mg, 4.24×10^{-4} mol, 69%). M.p. >250 °C; R_f = 0.42 (DCM/MeOH, 9:1); ^{1}H NMR (400 MHz, $CDCl_3$): δ = 7.48 – 7.40 (m, 3H, CH_{Ar}), 7.31 – 7.26 (m, 2H, CH_{Ar}), 5.99 (s, 2H $CH_{pyrrole}$), 3.25 (s, 4H, CH_2), 2.73 (s, 6H, $CH_{3pyrrole}$), 2.32 (s, 12H, NCH_3), 1.34 ppm (s, 6H, $CH_{3pyrrole}$); ^{13}C NMR (101 MHz, $CDCl_3$): δ = 154.8, 141.6, 140.9, 135.5, 129.5, 128.9, 128.6, 128.1, 121.4, 48.9, 44.0, 16.1, 14.5 ppm; UV/Vis (DCM): λ_{max} (log ε) = 500 nm (4.68); HRMS (ESI) *m/z* calcd. for $C_{29}H_{36}BN_4$ $[M+H]^+$: 451.3033, 451.3033 found.

1,3,5,7-(((Tetramethyl-8-(phenyl-9-yl)-4-bora-3a,4a-diaza-*s*-indacene-4,4-diyl)bis(prop-2-yne-3,1-diyl))bis(dimethylammoniumdiyl))bis(propane-1-sulfonate), 20: Compound **20** was synthesized in accordance with general procedure B using compound **28** (180 mg, 4.00×10^{-4} mol), in EtOAc (100 mL) and 1,3-propanesultone (296 mg, 2.40 mmol) to yield an orange solid (121 mg, 1.74×10^{-4} mol, 45%). M.p. >250 °C; ^{1}H NMR (400 MHz, DMSO-d_6): δ = 7.57 – 7.56 (m, 3H, CH_{Ar}), 7.43 – 7.31 (m, 2H, CH_{Ar}), 6.27 – 6.25 (m, 2H, $CH_{pyrrole}$), 4.33 – 4.30 (m, 4H, CH_2), 3.57 – 3.43 (m, 4H, CH_2), 3.07 (s, 12H, NCH_3), 2.69 – 2.68 (m, H, CH_3), 2.45 – 2.45 (m, 4H, CH_2), 2.15 – 1.95 (m, 4H, CH_2), 1.34 ppm (s, 6H, CH_3); ^{13}C NMR (101 MHz, DMSO-d_6): δ = 154.9, 154.7, 142.0, 142.0, 141.4, 141.0, 134.2, 134.1, 129.3, 127.8, 121.9, 121.0, 62.6, 62.6, 54.6, 55.5, 49.7, 49.6, 48.4, 47.4, 47.9, 47.8, 47.5, 44.7, 43.0, 28.9, 19.0, 15.9, 15.8, 14.1, 14.1 ppm; UV/Vis (DCM): λ_{max} (log ε) = 498 nm (4.49); HRMS (MALDI) *m/z* calcd. for $C_{35}H_{48}BN_4O_6S_2$ $[M+H]^+$: 695.3108, 695.3135 found.

Conflicts of interest

There are no conflicts to declare.

Acknowledgements

This work was supported by grants from the Science Foundation Ireland (IvP 13/IA/1894), the European Commission (CONSORT, Grant No. 655142) and the Irish Research Council (GOIPG/2016/1250).

Notes and references

‡ Quantum yields were measured using DPBF as a singlet oxygen trap and Rose Bengal or **BAD-6** as a reference photosensitizer.
§ Fluorescein in 0.1 M NaOH (ϕf = 0.95) was used as a reference for fluorescent quantum yields.

1 (a) T. J. Dougherty, C. J. Gomer, B. W. Henderson, G. Jori, D. Kessel, M. Korbelik, J. Moan and Q. Peng, Photodynamic therapy, *J. Natl. Cancer Inst*., 1998, **90**, 889–905; (b) B. W. Henderson and T. J. Dougherty, How does photodynamic therapy work?, *Photochem. Photobiol.*, 1992, **55**, 1, 145–57.

2 (a) S. B. Brown, E. A. Brown and I. Walker, The present and future role of photodynamic therapy in cancer treatment, *Lancet Oncol*., 2004, **5**, 497–508; (b) X. Wen, Y. Li and M. R. Hamblin, Photodynamic therapy in dermatology beyond non-melanoma cancer: an update, *Photodiagn. Photodyn. Ther.,* 2017, **19**, 140–152; (c) U. Schmidt-Erfurth and T. Hasan, Mechanisms of action of photodynamic therapy with verteporfin for the treatment of age-related macular degeneration, *Surv. Ophthalmol*., 2000, **45**, 195–214; (d) M. R. Hamblin and T. Hasan, Photodynamic therapy: a new antimicrobial approach to infectious disease?, *Photochem. Photobiol. Sci*., 2004, **3**, 436–450.

3 (a) A. Treibs and F.-H. Kreuzer, Difluorboryl-Komplexe von Di- und Tripyrrylmethenen, *Justus Liebigs Ann. Chem.*, 1968, **718**, 208–223; (b) A. Kamkaew, S. Hui Lim, H. B. Lee, L. V. Kiew, L. Y. Chung and K. Burgess, BODIPY dyes in photodynamic therapy, *Chem. Soc. Rev.*, 2013, **42**, 77–88.

4 S. Callaghan and M. O. Senge, The good, the bad, and the ugly –controlling singlet oxygen through design of photosensitizers and delivery systems for photodynamic therapy, *Photochem. Photobiol. Sci*., 2018, **17**, 1490–1514.

5 A. Loudet and K. Burgess, BODIPY dyes and their derivatives: syntheses and spectroscopic properties, *Chem. Rev*., 2007, **107**, 4891–4932.

6 S. Banfi, E. Caruso, S. Zaza, M. Mancini, M. B. Gariboldi and E. Monti, Synthesis and photodynamic activity of a panel of BODIPY dyes, *J. Photochem. Photobiol. B: Biol*., 2012, **114**, 52–60.

7 W. Pang, X.-F. Zhang, J. Zhou, C. Yu, E. Hao and L. Jiao, Modulating the singlet oxygen generation property of meso–β directly linked BODIPY dimer, *Chem. Commun*., 2012, **48**, 5437–5439.

8 W. Wu, J. Zhao, J. Sun and S. Guo, Light-harvesting fullerene dyads as organic triplet photosensitizers for triplet–triplet annihilation upconversions, *J. Org. Chem.,* 2012, **77**, 5305–5312.

9 (a) A. Gorman, J. Killoran, C. O'Shea, T. Kenna, W. M. Gallagher and D. F. O'Shea, In vitro demonstration of the heavy-atom effect for photodynamic therapy, *J. Am. Chem. Soc.*, 2004, **126**, 34, 10619–10631; (b) A. T. Byrne, A. E. O'Connor, M. Hall, J. Murtagh, K. O'Neill, K. M. Curran, K. Mongrain, J. A. Rousseau, R. Lecomte, S. McGee, J. J. Callanan, D. F. O'Shea and W. M. Gallagher, Vascular-targeted photodynamic therapy with BF2-chelated Tetraaryl-Azadipyrromethene agents: a multi-modality molecular imaging approach to therapeutic assessment, *Br. J. Cancer*, 2009, **101**, 1565–1573.

10 (a) M. A. Filatov, S. Karuthedath, P. M. Polestshuk, H. Savoie, K. J. Flanagan, C. Sy, E. Sitte, M. Telitchko, F. Laquai, R. W. Boyle and M. O. Senge, Generation of Triplet Excited States via Photoinduced Electron Transfer in meso-anthra-BODIPY: Fluorogenic Response toward Singlet Oxygen in Solution and in Vitro, *J. Am. Chem. Soc*., 2017, **139**, 6282–6285; (b) M. A. Filatov, S. Karuthedath, P. M. Polestshuk, S. Callaghan, K. J. Flanagan, M. Telitchko, T. Wiesner, F. Laquaic and M. O. Senge, Control of triplet state generation in heavy atom-free BODIPY–anthracene dyads by media polarity and structural factors, *Phys. Chem. Chem. Phys.,* 2018, **20**, 8016–8031; (c) M. A. Filatov, S. Karuthedath, P. M. Polestshuk, S. Callaghan, T. Wiesner, K. J. Flanagan, F. Laquai and M. O. Senge, BODIPY-Pyrene and Perylene Dyads as Heavy-Atom-Free Singlet Oxygen Sensitizers, *ChemPhotoChem*, 2018, **2**, 1–11.

11 (a) M. R. Wasielewski, Photoinduced electron transfer in supramolecular systems for artificial photosynthesis, *Chem. Rev.,* 1992, **92**, 435–461; (b) T. Kowada, H. Maeda, K. Kikuchi, BODIPY-based probes for the fluorescence imaging of biomolecules in living cells, *Chem. Soc. Rev.*, 2015, **44**, 4953–4972.

12 N. Kiseleva, M. A. Filatov, M. Oldenburg, D. Busko, M. Jakoby, I. A. Howard, B. S. Richards, M. O. Senge, S. M. Borisov, A. Turshatov, The Janus-faced chromophore: a donor–acceptor dyad with dual performance in photon up-conversion, *Chem. Commun.* 2018, **54**, 1607–1610.
13 S. L. Niu, G. Ulrich, R. Ziessel, A. Kiss, P.-Y. Renard and A. Romieu, Water-soluble BODIPY derivatives, *Org. Lett.,* 2009, **11**, 2049–2052.
14 J. R. Lakowicz, Principles of Fluorescence Spectroscopy, 2nd Ed., Kluwer Academic/Plenum Publishers, New York, London, Moscow, Dordrecht, 1999.
15 Y. Cakmak, S. Kolemen, S. Duman, Y. Dede, Y. Dolen, B. Kilic, Z. Kostereli, L. T. Yildirim, A. L. Dogan, D. Guc, E. U. Akkaya, Designing Excited States: Theory-Guided Access to Efficient Photosensitizers for Photodynamic Action, *Angew. Chem. Int. Ed.,* 2011, **50**, 11937–11941.
16 T. Mosman, Rapid colorimetric assay for cellular growth and survival: application to proliferation and cytotoxicity assays, *J. Immunol. Methods,* 1983, **65**, 55–63.
17 J.-M. Aubry, C. Pierlot, J. Rigaudy and R. Schmidt, *Acc. Chem. Res.*, 2003, **36**, 668−675.
18 (a) D. V. Ash and B. Brown, New drugs and future developments in photodynamic therapy, *Eur. J. Cancer*, 1983, **29**, 1781−1783; (b) S.-I. Moriwaki, J. Misawa, Y. Yoshinari, I. Yamada, M. Takigawa and Y. Tokura, Analysis of photosensitivity in Japanese cancer-bearing patients receiving photodynamic therapy with porfimer sodium (PhotofrinTM), *Photodermatol. Photoimmunol. Photomed*., 2001, **17**, 241–243.
19 H. Sunahara, Y. Urano, H. Kojima and T. Nagano, Design and synthesis of a library of BODIPY-based environmental polarity sensors utilizing photoinduced electron-transfer-controlled fluorescence ON/OFF switching, *J. Am. Chem. Soc*., 2007, **129**, 5597–5604.
20 P. A. Liddell, T. P. Forsyth, M. O. Senge and K. M. Smith, Chemical synthesis of a “GSA-pyrrole” and its reaction with Ehrlich's reagent, *Tetrahedron*, 1993, **49**, 1343–1350.
21 M. A. Filatov, R. Guilard and P. D. Harvey, Selective Stepwise Suzuki Cross-Coupling Reaction for the Modelling of Photosynthetic Donor− Acceptor Systems, *Org. Lett.*, 2010, **12**, 196–199.
22 Y. Gabe, Y. Urano, K. Kikuchi, H. Kojima and T. Nagano, Highly sensitive fluorescence probes for nitric oxide based on boron dipyrromethene chromophore rational design of potentially useful bioimaging fluorescence probe, *J. Am. Chem. Soc*., 2004, **126**, 3357–3367.

ToC graphic

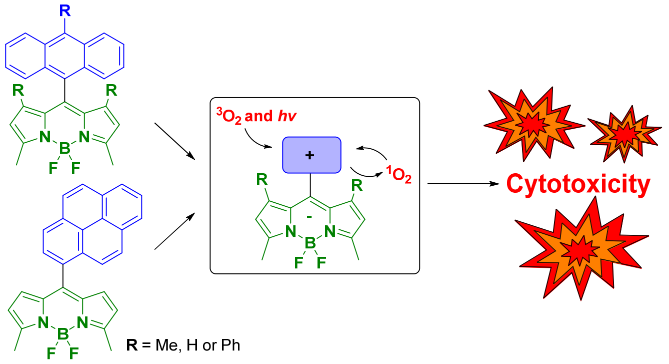

ToC text entry

A library of heavy atom-free BODIPY-anthracene and -pyrene dyads capable of generating singlet oxygen *via* a PeT mechanism have been synthesized and their *in vitro* activity has been demonstrated.